
Recovering Petaflops in Contrastive Semi-Supervised Learning of Visual Representations

Mahmoud Assran^{1,2,3}, Nicolas Ballas³, Lluís Castrejon^{1,3,4}, and Michael Rabbat^{1,3}

¹Mila – Quebec AI Institute

²Department of Electrical and Computer Engineering, McGill University

³Facebook AI Research

⁴Department of Computer Science and Operations Research, University of Montreal
{massran, ballasn, lcastrejon, mikerabbat}@fb.com

Abstract

We investigate a strategy for improving the computational efficiency of contrastive learning of visual representations by leveraging a small amount of supervised information during pre-training. We propose a semi-supervised loss, SuNCeT, based on noise-contrastive estimation, that aims to distinguish examples of different classes in addition to the self-supervised instance-wise pretext tasks. We find that SuNCeT can be used to match the semi-supervised learning accuracy of previous contrastive approaches with significantly less computational effort. Our main insight is that leveraging even a small amount of labeled data during pre-training, and not only during fine-tuning, provides an important signal that can significantly accelerate contrastive learning of visual representations.

1 Introduction

Learning visual representations that are semantically meaningful with limited semantic annotations is a longstanding challenge with the potential to drastically improve the data-efficiency of learning agents. Semi-supervised learning algorithms based on contrastive instance-wise pretext tasks learn representations with limited label information and have shown great promise [19, 49, 2, 33, 7]. Unfortunately, despite achieving state-of-the-art performance, these semi-supervised contrastive approaches typically require at least an order of magnitude more compute than standard supervised training with a cross-entropy loss (albeit without requiring access to the same amount of labeled data). Burdensome computational requirements not only make training laborious and particularly time- and energy-consuming; they also exacerbate other issues, making it more difficult to scale to more complex models and problems, and potentially inducing significant carbon footprints depending on the infrastructure used for training [22].

In this work, we investigate a strategy for improving the computational efficiency of contrastive learning of visual representations by leveraging a small amount of supervised information during pre-training. We propose a semi-supervised loss, SuNCeT, based on noise-contrastive estimation [18], that aims at distinguishing examples of different classes in addition to the self-supervised instance-wise pretext tasks. We conduct a case-study with respect to the state-of-the-art approach of Chen et al. [7] on the ImageNet [38] and CIFAR10 [27] benchmarks. We find that SuNCeT can be used to match the semi-supervised learning accuracy of previous contrastive approaches while recovering petaflops of computation in the process.

2 Background on self-supervised contrastive learning

The goal of contrastive learning is to learn representations by comparison. Recently, this class of approaches has fueled rapid progress in unsupervised representation learning of images through self-supervision [8, 19, 2, 36, 21, 46, 33, 20, 1, 7]. In that context, contrastive approaches usually learn by maximizing the agreement between representations of different views of the same image. Many self-supervised contrastive learning methods utilize instance-wise approaches and perform pairwise comparison of input data to push representations of similar inputs close to one another while pushing apart representations of dissimilar inputs, akin to a form of distance-metric learning.

Self-supervised contrastive approaches typically rely on a data-augmentation module, an encoder network, and a contrastive loss. The data augmentation module stochastically maps an image $x_i \in \mathbb{R}^{3 \times H \times W}$ to a different view. Denote by $\hat{x}_{i,1}, \hat{x}_{i,2}$ two possible views of an image x_i , and denote by f_θ the parameterized encoder, which maps an input image $\hat{x}_{i,1}$ to a representation vector $z_{i,1} = f_\theta(\hat{x}_{i,1}) \in \mathbb{R}^d$. The encoder f_θ is usually parameterized as a deep neural network with learnable parameters θ . Given a representation $z_{i,1}$, referred to as an anchor embedding, and the representation of an alternative view of the same input $z_{i,2}$, referred to as a positive sample, the goal is to optimize the encoder f_θ to output representations that enable one to easily discriminate between the positive sample and noise using multinomial logistic regression. This learning by picking out the positive sample from a pool of negatives is in the spirit of noise-contrastive estimation [18]. The noise samples in this context are often taken to be the representations of other images. For example, suppose we have a set of images $(x_i)_{i \in [n]}$ and apply the stochastic data-augmentation to construct a new set with two views of each image, $(\hat{x}_{i,1}, \hat{x}_{i,2})_{i \in [n]}$. Denote by $\mathcal{Z} = (z_{i,1}, z_{i,2})_{i \in [n]}$ the set of representations corresponding to these augmented images. Then the noise samples with respect to the anchor embedding $z_{i,1} \in \mathcal{Z}$ are given by $\mathcal{Z} \setminus \{z_{i,1}, z_{i,2}\}$. In this work, we minimize the normalized temperature-scaled cross entropy loss [42, 7] for instance-wise discrimination

$$\ell_{\text{inst}}(z_{i,1}) = -\log \frac{\exp(\text{sim}(z_{i,1}, z_{i,2})/\tau)}{\sum_{z \in \mathcal{Z} \setminus \{z_{i,1}\}} \exp(\text{sim}(z_{i,1}, z)/\tau)}, \quad (1)$$

where $\text{sim}(a, b) = \frac{a^T b}{\|a\| \|b\|}$ denotes the cosine similarity and $\tau > 0$ is a temperature parameter.

In typical semi-supervised contrastive learning setups, the encoder f_θ is learned in a fully unsupervised pre-training procedure. The goal of this pre-training is to learn a representation invariant to common data augmentations (cf. [19, 33]) such as random crop/flip, resizing, color distortions, and Gaussian blur. After pre-training on unlabeled data, labeled training instances are leveraged to fine-tune f_θ , e.g., using the canonical cross-entropy loss.

3 Semi-supervised contrastive learning methodology

Our goal is to investigate a strategy for improving the computational efficiency of contrastive learning of visual representations by leveraging the available supervised information during pre-training. We explore a contrastive approach for utilizing available labels.

Semi-supervised noise contrastive estimation. Consider a set \mathcal{S} of labeled samples operated upon by the stochastic data-augmentation module. The associated set of parameterized embeddings are given by $\mathcal{Z}_\mathcal{S}(\theta) = (f_\theta(\hat{x}))_{\hat{x} \in \mathcal{S}}$. Let \hat{x} denote an anchor image view with representation $z = f_\theta(\hat{x})$ and class label y . By slight overload of notation, denote by $\mathcal{Z}_y(\theta)$ the set of embeddings for images in \mathcal{S} with class label y (same class as the anchor z). We define the *Supervised Noise Contrastive Estimation* (SuNCEt) loss as

$$\ell(z) = -\log \frac{\sum_{z_j \in \mathcal{Z}_y(\theta)} \exp(\text{sim}(z, z_j)/\tau)}{\sum_{z_k \in \mathcal{Z}_\mathcal{S}(\theta) \setminus \{z\}} \exp(\text{sim}(z, z_k)/\tau)}. \quad (2)$$

In each iteration of training we sample a few images for which class labels are available, as well as a few unlabeled images; we use the labeled images to compute the SuNCEt loss (2), and use the unlabeled images to compute the self-supervised instance-wise loss (1). We sum these two losses together and backpropagate through the encoder network. By convention, when “sampling unlabeled images,” we actually sample images from the entire training set (labeled and unlabeled).

Motivation. We motivate the form of the SuNCEt loss by leveraging the relationship between contrastive representation learning and distance-metric learning. Consider a classifier that predicts an image’s class based on the distance of the image’s embedding z to those of other labeled images z_j using a temperature-scaled cosine similarity distance metric $d(z, z_j) = z^T z_j / (\|z\| \|z_j\| \tau)$. Specifically, let the classifier randomly choose one point as its neighbour, with distribution as described below, and adopt the neighbour’s class. Given the query embedding z , denote the probability that the classifier selects point $z_j \in \mathcal{Z}_S(\theta) \setminus \{z\}$ as its neighbour by

$$p(z_j|z) = \frac{\exp(d(z, z_j))}{\sum_{z_k \in \mathcal{Z}_S(\theta) \setminus \{z\}} \exp(d(z, z_k))}.$$

Under mutual exclusivity (since the classifier only chooses one neighbour) and a uniform prior, the probability that the classifier predicts the class label \hat{y} equal to some class c , given a query image x with embedding z , is

$$p(\hat{y} = c|z) = \sum_{z_j \in \mathcal{Z}_c(\theta)} p(z_j|z) = \frac{\sum_{z_j \in \mathcal{Z}_c(\theta)} \exp(d(z, z_j))}{\sum_{z_k \in \mathcal{Z}_S(\theta) \setminus \{z\}} \exp(d(z, z_k))},$$

where $\mathcal{Z}_c(\theta) \subset \mathcal{Z}_S(\theta)$ is the set of embeddings of labeled images from class c . Minimizing the KL divergence between $p(\hat{y}|z)$ and the true class distribution (one-hot vector on the true class y), one arrives at the SuNCEt loss in (2). Assuming independence between labeled samples, the aggregate loss with respect to all labeled samples \mathcal{S} decomposes into the simple sum $\sum_{z \in \mathcal{Z}_S(\theta)} \ell(z)$. The relation to previous work on contrastive supervised learning is discussed in Section 5.

3.1 Practical considerations

In practice, we use one data loader for sampling mini-batches of images to compute the instance-discrimination loss (1), and another data loader for sampling mini-batches of (labeled) images to compute the SuNCEt loss (2). When there are too many image classes to contrast at once, we randomly subsample a set of classes, and then sample a set of images from each subsampled class to construct the supervised mini-batch. We also average the stochastic estimate of the SuNCEt loss over all images (anchors) in our mini-batch. We adopt the stochastic data-augmentation strategy from [7] for all labeled images.

For distributed training, there may not be enough labeled samples in each class to parallelize computation of SuNCEt across all workers, and so the set $\mathcal{Z}_y(\theta)$ in (2) may contain embeddings originating from the same image, but with different random transformations, in which case, the SuNCEt loss can be seen as a semi-supervised extension of instance-discrimination.

Lastly, rather than directly using the outputs of encoder f_θ to contrast samples, we feed the representations into a small multi-layer perceptron (MLP), $h_{\theta_{\text{proj}}}$, to project the representations into a lower dimensional subspace before evaluating the contrastive loss, following [7]. That is, instead of using $z = f_\theta(\hat{x})$ directly in (1) and (2), we use $h_{\theta_{\text{proj}}}(z) = h_{\theta_{\text{proj}}}(f_\theta(\hat{x}))$. The projection network $h_{\theta_{\text{proj}}}$ is only used for optimizing the contrastive loss, and is discarded at the fine-tuning phase.

4 Experiments

In this section, we investigate the computational effects of SuNCEt when combined with the SimCLR self-supervised instance-wise pretext task defined in Section 2.¹ SimCLR [7] establishes the current state-of-the-art for contrastive semi-supervised learning of visual representations. We report results on the ImageNet [38] and CIFAR10 [27] benchmarks for comparison with related work. All methods are trained for a default of 500 epochs using the LARS optimizer [51] along with a cosine-annealing learning-rate schedule [31]. Results reported at intermediate epochs correspond to checkpoints from these 500 epochs training runs, and are intended to illustrate training dynamics.

The standard procedure when evaluating semi-supervised learning methods on these data sets is to assume that some percentage of the data is labeled, and treat the rest of the data as unlabeled. On ImageNet we directly use the same 1% and 10% data splits used in [7]. On CIFAR10, we create the labeled data sets by independently selecting each point to be in the set of labeled training points with some probability p ; we run experiments for each p in $\{0.01, 0.05, 0.1, 0.2, 0.5, 1.0\}$.

¹The SuNCEt loss can certainly be combined with other instance-wise pretext tasks as well.

Architecture & data. The encoder network in our experiments is a ResNet-50. On CIFAR10 we modify the trunk of the encoder following [7]. While this network may not be optimal for CIFAR10 images, it enables fair comparison with previous work. For the projection network $h_{\theta_{\text{proj}}}$ we use an MLP with a single hidden-layer; the hidden layer has 2048 units and the output of the projection network is a 128-dimensional real vector. The stochastic data augmentation module employs random cropping, random horizontal flips, and color jitter. On ImageNet, we also make use of Gaussian blur.

Fine-tuning. Upon completion of pre-training, all methods are fine-tuned on the available set of labeled data using SGD with Nesterov momentum [44]. We adopt the same fine-tuning procedure as Chen et al. [7]. Notably, when fine-tuning, we do not employ weight-decay and only make use of basic data augmentations (random cropping and random horizontal flipping). Additional details on the fine-tuning procedure are provided in the appendix.

4.1 CIFAR10

Experimental setup. Our training setup on CIFAR10 uses a single V100 GPU and 10 CPU cores. We use a learning-rate of 1.0, momentum 0.9, weight decay 10^{-6} , and temperature 0.5. These hyper-parameters are tuned for SimCLR [7], and we also apply them to the SimCLR + SuNCEt combination.

We use a batch-size of 256 (512 contrastive samples) for SimCLR. When implementing the SimCLR + SuNCEt combination, we set out to keep the cost per-iteration roughly the same as the baseline, so we use a smaller unsupervised batch-size of 128 (256 contrastive samples) and use a supervised batch-size of 280 (sampling 28 images from each of the 10 classes in the labeled data set), for a total of 536 labeled+unlabeled images to be sampled in each iteration. Note that we only sample images from the available set of labeled data to compute the SuNCEt loss in each iteration.

We turn off the penalty after the first 100 epochs and revert back to completely self-supervised learning for the remaining 400 epochs of pre-training to avoid overfitting to the small fraction of available labeled data; we elaborate on this point in Section 4.3. The only exception to this rule is the set of experiments where 100% of the training data is labeled, in which case we keep SuNCEt on for the entire 500 epochs.

Results. Figure 1a shows the convergence of SimCLR with various amounts of labeled data, both in terms of epochs (left sub-figure) and in terms of computation (right sub-figure). Both the sample efficiency and computational efficiency of SimCLR improve with the availability of labeled data, even if labeled data is only used for fine-tuning.

Figure 1b shows the convergence of the SimCLR + SuNCEt combination with various amounts of labeled data, both in terms of epochs (left sub-figure) and in terms of computation (right sub-figure). Epochs are counted with respect to the number of passes through the unsupervised data-loader. We observe a similar trend in the SimCLR + SuNCEt combination, where both the sample efficiency and computational efficiency improve with the availability of labeled data.

Making use of SuNCEt also improves the sample efficiency of SimCLR. Figure 1c shows the improvement in Top 1 test accuracy throughout training (relative to SimCLR) when using SuNCEt. Not only does SuNCEt accelerate training from a sample efficiency point of view, but it also leads to better models at the end of training.

Figure 1c shows acceleration from a sample efficiency point of view, however, it is more difficult to tease apart computational advantages from it. While the cost-per-iteration for both methods is roughly the same, the use of a smaller self-supervised batch-size means we perform more iterations per epoch when using SimCLR + SuNCEt. In particular, the SimCLR + SuNCEt curve with 100% labeled data in the right subplot of Figure 1b uses much more compute during the 500 training epochs than the other trials as the SuNCEt loss is kept on for the entire training. To address the difference in the computational cost per epoch, Figure 1d shows the amount of computation saved by the SimCLR + SuNCEt combination in reaching the best SimCLR accuracy. There are two x-axes in this figure. The top shows the petaflops saved and the bottom shows the number of model updates saved to reach the best SimCLR test accuracy. SuNCEt saves computation for any given amount of supervised samples.

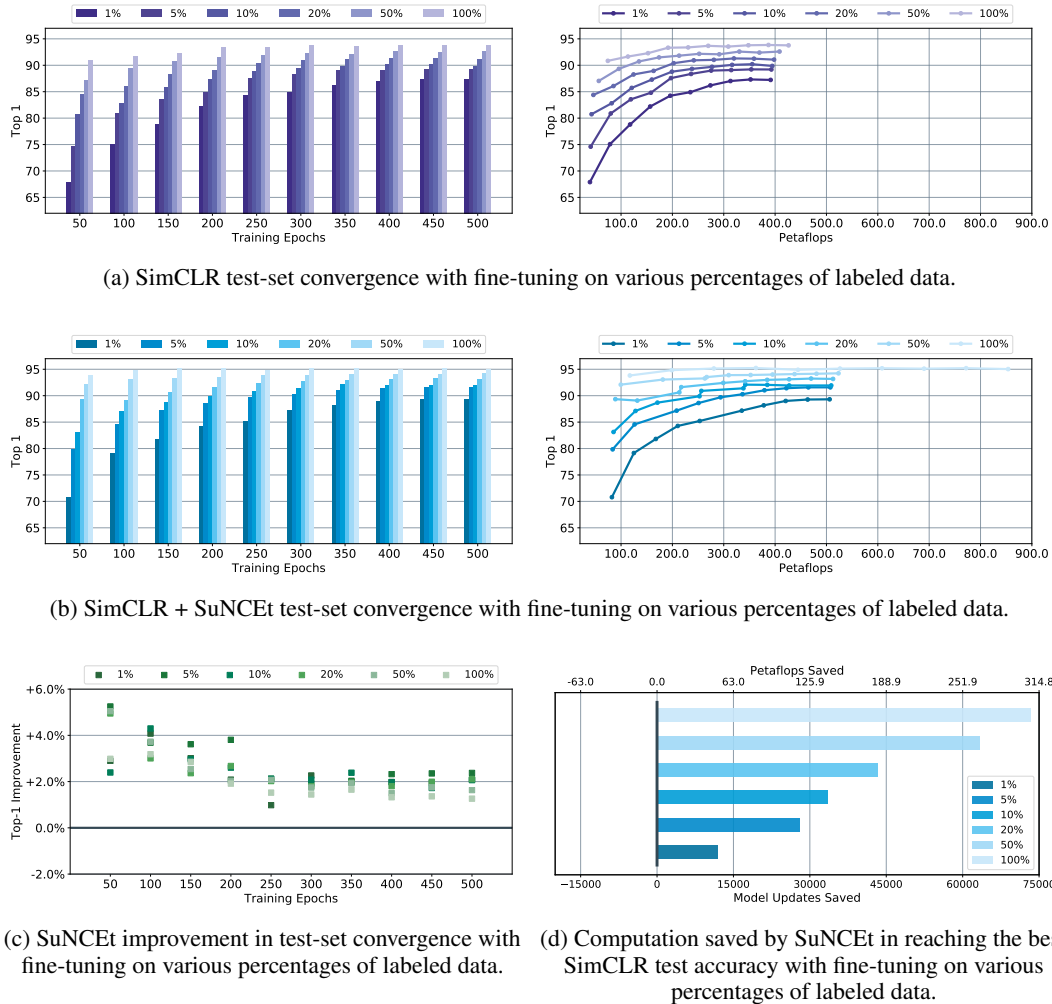


Figure 1: Training a ResNet50 with an adjusted-stem on CIFAR10 given various percentages of labeled data. Evaluations reported at intermediate epochs correspond to checkpoints from the same run, with a 500 epoch learning-rate cosine-decay schedule. SuNCEt epochs are counted with respect to number of passes through the unsupervised data loader.

With only 1% of the training data labeled, SuNCEt can reach the best SimCLR test accuracy while conserving roughly 50 petaflops of computation and over 10000 model updates.²

4.2 ImageNet

Experimental setup. Our default setup on ImageNet makes use of distributed training; we train each run on 64 V100 GPUs and 640 CPU cores. We aggregate gradients using the standard all-reduce primitive and contrast representations across workers using an efficient all-gather primitive. We also synchronize batch-norm statistics across all workers in each iteration to prevent the models from leaking local information to improve the loss without improving representations (cf. Chen et al. [7]). We linearly warm-up the learning-rate from 0.6 to 4.8 during the first 10 epochs of training and use a cosine-annealing schedule thereafter. We use a momentum value of 0.9, weight decay 10^{-6} , and temperature 0.1. Similar to the experiments on CIFAR10, these hyper-parameters are tuned for SimCLR [7], but we also apply them to the SimCLR + SuNCEt combination.

²One model update refers to the process of completing a forward-backward pass, computing the loss, and performing an optimization step.

We use a batch-size of 4096 (8192 contrastive samples) for SimCLR. When implementing the SimCLR + SuNCEt combination, we again aim to keep the cost per-iteration roughly the same as the baseline, so we use a smaller unsupervised batch-size. Specifically, when 10% of the training data is labeled we use an unsupervised batch-size of 2048 (4096 contrastive samples) and use a supervised batch-size of 5120 (sub-sampling 40 classes in each iteration and sampling 128 images from each of the sub-sampled classes), for a total of 7168 labeled/unlabeled images to be sampled in each iteration. Similar to our previous set of experiments, we turn off the SuNCEt loss after epoch 100.

When only 1% of data is labeled, we use an unsupervised batch-size of 2880 (5760 contrastive samples) and use a supervised batch-size of 3200 (sub-sampling 25 classes in each iteration and sampling 128 images from each of the sub-sampled classes), for a total of 8960 labeled/unlabeled images to be sampled in each iteration. We turn off the SuNCEt loss after epoch 30, and revert to purely self-supervised learning thereafter. As mentioned in Section 3.1, not all of the sampled labeled images used to compute the SuNCEt loss are unique. Many of the samples in the supervised mini-batch correspond to the same image but with different random augmentations (in fact, for the 1% labeled data setting, there are roughly 12 labeled images per class).

Results. Table 1 reports the single-crop Top-1 and Top-5 validation accuracy of various semi-supervised representation learning methods when 10% of the training data is labeled. Table 2 reports similar results, but when only 1% of the training data is labeled. Although it is not the focus of this work, we observe that the SimCLR + SuNCEt combination, with the default SimCLR hyperparameters, outperforms all other contrastive methods, including the vanilla SimCLR protocol of fully unsupervised pretraining followed by fine-tuning, on both the 1% and 10% data splits. We observe that when 10% of training data is labeled, the SimCLR validation performance saturates; training for 1000 epochs instead of 500 epochs only provides a marginal 0.4% to 0.5% boost in performance. When 1% of the training data is labeled, training SimCLR for 1000 epochs instead of 500 epochs actually degrades performance on the validation set.

Table 3 reports the amount of computation save by the SimCLR + SuNCEt combination in reaching the best SimCLR validation accuracy. Table 4 reports similar results, but when only 1% of the training data is labeled. When 10% of the training data is labeled, SimCLR + SuNCEt reaches the best 500 epoch SimCLR Top-1 validation accuracy while conserving roughly 1900 petaflops and 9200 model updates, and reaches the best 500 epoch SimCLR Top-5 validation accuracy while conserving roughly 3900 petaflops and 19400 model updates. The improvements with respect to 1000 epoch SimCLR baseline are even more stark. SimCLR + SuNCEt reaches the best 1000 epoch SimCLR Top-1 validation accuracy while conserving roughly 33100 petaflops and 164000 model updates, and reaches the best 1000 epoch SimCLR Top-5 validation accuracy while conserving roughly 23700 petaflops and 117300 model updates. When 1% of the training data is labeled, we still see improvements in the computational effort utilized to reach the best 500 epoch SimCLR Top-1 and Top-5 validation accuracy, namely conserving roughly 2100 petaflops and 10000 model updates to reach the best 500 epoch SimCLR Top-1 validation accuracy, and saving roughly 5500 epochs and 27000 updates to reach the best 500 epoch SimCLR Top-5 validation accuracy.

4.3 Limitations

As it is shown in Figure 1d, the ability of the SuNCEt loss to improve the computational efficiency of training and recover petaflops of computation is highly correlated to the amount of labeled data. In the limit where there are only a few labeled data points, we cannot expect SuNCEt to provide any significant advantages over pure instance-wise discrimination. One research direction to overcome this limitation would be the use of label-propagation [29, 5] or cluster prototypes [41, 30] to make use of unlabeled data in the SuNCEt loss.

Another limitation of the SuNCEt loss is that we must turn it off at some point during training. On CIFAR10 we observe that using SuNCEt for too long can lead to overfitting and degrade performance. The amount of time that we can leave SuNCEt on without degrading performance is positively correlated with the amount of available labeled data (see the appendix). Similarly on ImageNet, we observe that the most computationally efficient trials are obtained by turning off SuNCEt early on in training. In that regard, the SuNCEt loss serves as a bootstrap at the start of training, the benefits of which remain even after the loss has been turned off. In practice, we turn off SuNCEt when it flattens out.

Table 1: ImageNet with ResNet-50 encoder when 10% of training data is labeled. We compare performance of contrastive semi-supervised approaches with our method (second block). Compared to SimCLR, the state-of-the-art contrastive approach, SuNCEt reaches better accuracy while reducing computation. We also report performance of approaches based on label propagation (first block) that achieve the best performance on this task. *SuNCEt epochs are counted with respect to number of passes through the unsupervised data loader.

10% Labeled			Accuracy (%)	
Method	Training Epochs	Petaflops	Top 1	Top 5
<i>Non-contrastive methods using label-propagation:</i>				
UDA [50] (+ Rand.Augment [9])	–	–	68.8	88.8
FixMatch [43] (+ Rand.Augment [9])	–	–	71.5	89.1
<i>Contrastive methods using representation learning only:</i>				
NPID [49]	200	–	–	77.4
NPID++ [33, 49]	800	–	–	81.5
PIRL [33]	800	–	–	83.8
SimCLR [7]	1000	~63200	65.6	87.8
SimCLR	500	~31600	65.4	87.3
+ SuNCEt (ours)	500	~39500	66.3	87.9

Table 2: ImageNet with ResNet-50 encoder. Semi-supervised performance (with reported compute) when 1% of training data is labeled. Comparing to other contrastive semi-supervised representation learning methods. *SuNCEt epochs are counted with respect to number of passes through the unsupervised data loader.

1% Labeled			Accuracy (%)	
Method	Training Epochs	Petaflops	Top 1	Top 5
NPID [49]	200	–	–	39.2
NPID++ [33, 49]	800	–	–	52.6
PIRL [33]	800	–	–	57.2
SimCLR [7]	1000	~63100	48.3	75.5
SimCLR	500	~31500	49.4	76.9
+ SuNCEt (ours)	500	~32600	49.5	77.3

Table 3: ImageNet with ResNet-50 encoder. Computation saved by SuNCEt in reaching the best Top 1 and Top 5 validation accuracy achieved by SimCLR with 500 and 1000 epochs of training when 10% of training data is labeled. *Updates saved reported across all workers with a batch-size of 4096 (8192 contrastive samples) partitioned across 64 V100 GPUs.

10% Labeled	Target Acc.		Top 1 (Compute Saved)		Top 5 (Compute Saved)	
	Top 1	Top 5	Petaflops	Updates	Petaflops	Updates
SimCLR Pretraining						
500 epochs	65.4	87.3	~1900	9248	~3900	19437
1000 epochs	65.6	87.8	~33100	164009	~23700	117353

Table 4: ImageNet with ResNet-50 encoder. Computation saved by SuNCEt in reaching the best Top 1 and Top 5 validation accuracy achieved by SimCLR with 500 epochs of training when 1% of training data is labeled. *Updates saved reported across all workers with a batch-size of 4096 (8192 contrastive samples) partitioned across 64 V100 GPUs.

1% Labeled	Target Acc.		Top 1 (Compute Saved)		Top 5 (Compute Saved)	
	Top 1	Top 5	Petaflops	Updates	Petaflops	Updates
SimCLR Pretraining						
500 epochs	49.4	76.9	~2100	10392	~5500	27002

5 Related work

Self-supervised learning. There are a number of other self-supervised learning approaches in the literature, besides the instance-discrimination pretext task in SimCLR [7]. Some non-contrastive approaches learn feature representations by relative patch prediction [12], by solving jigsaws [35], by applying and predicting image rotations [15], by inpainting or colorization [10, 37, 53, 54], by parametric instance-discrimination [13], and sometimes by combinations thereof [11, 26]. Of the contrastive approaches, Contrastive Predictive Coding (CPC) [36, 21] compares representations from neighbouring patches of the same image to produce representations with a local regularity that are discriminative of particular samples. Non-Parametric Instance Discrimination (NPID) [49] aims to learn representations that enable each input image to be uniquely distinguished from the others, and makes use of a memory bank to train with many contrastive samples. The NPID training objective offers a non-parametric adaptation of Exemplar CNN [13]. Misra and van der Maaten [33] generalize the NPID method as Pretext-Invariant Representation Learning (PIRL) to contrast images both with and without data augmentations, and combine the method with other instance-wise pretext tasks. He et al. [20] propose Momentum Contrast (MoCo) to build even larger memory banks by using an additional slowly progressing key encoder, thus benefiting from more contrastive samples while avoiding computational issues with large-batch training. There is also the recent work [30], which makes use of EM [32] and clustering algorithms for estimating cluster prototypes [41].

Semi-supervised learning. Self-supervised learning methods are typically extended to the semi-supervised setting by fine-tuning the model on the available labeled data after completion of self-supervised pre-training. A recent exception to this general procedure is the S4L approach by Zhai et al. [52], which uses a cross-entropy loss during self-supervised pre-training. While that work does not study contrastive approaches, nor the computational efficiency of their method, they show that S4L can be combined in a stage-wise approach with other semi-supervised methods such as Virtual Adversarial Training [34], Entropy Regularization [17], and Pseudo-Label [29] to improve the final accuracy of their model (see follow-up work [47, 23]). Note that in [7], the SimCLR approach with self-supervised pretraining and supervised fine-tuning is reported to outperform the strong baseline combination of S4L with other semi-supervised tasks. Other semi-supervised learning methods not based on self-supervised learning include Unsupervised Data Augmentation (UDA) [50] and the MixMatch trilogy of work [4, 3, 43]. FixMatch [43] makes predictions on weakly augmented images and (when predictions are confident enough) uses those predictions as labels for strongly augmented views of those same images. An additional key feature of FixMatch is the use of learned data augmentations [3, 9]. Of the non-contrastive methods, FixMatch sets the current state-of-the-art on established semi-supervised learning benchmarks.

Supervised contrastive loss functions. Supervised contrastive losses have a rich history in the distance-metric learning literature. Classically, these methods utilized triplet losses [6, 24, 39] or max-margin losses [48, 45], and required computationally expensive hard-negative mining [40] or adversarially-generated negatives [14] in order to obtain informative contrastive samples that reveal information about the structure of the data. One of the first works to overcome expensive hard-negative mining was [42] (inspired from Neighbourhood Component Analysis [16]), which suggested using several negative samples per anchor. Another more recent supervised contrastive loss is that proposed in [25] for the fully supervised setting; while the method proposed in [25] is more computationally draining than training with a standard cross-entropy loss, it is shown to improve model robustness. The SuNCEt loss in this paper takes on a strictly different form from these aforementioned losses.

6 Conclusion

We have proposed a principled semi-supervised loss based on noise-contrastive estimation, and demonstrated how this loss can be used to recover petaflops of computation in matching the semi-supervised learning accuracy of previous contrastive approaches. While the proposed method outperforms other contrastive baselines, our work looks at how supervised information can be used to improve computational efficiency as opposed to the more classical study of model accuracy.

Broader Impact

Semi-supervised contrastive learning methods are used in many present-day applications to train models on large-scale data sets without requiring many semantic annotations. Though data-efficient, these approaches are very computationally intensive. It is essential to address the computational limitations of existing methods, not just to enable scaling to more complex tasks, but to also become more cognizant of the environmental cost of machine learning experiments, since petaflops can be directly connected to measures of energy (e.g., kWh) [28].

This work demonstrates that a small amount of supervised information leveraged during self-supervised pre-training (not just during fine-tuning) can quantitatively improve the computational efficiency of contrastive learning of visual representations. New methods rethinking the role of labeled information in self-supervised training pipelines — to not only improve model accuracy, but to also improve computational efficiency — can potentially lead to new approaches taking greater strides towards addressing the computational limitations of existing methods.

We are uncertain of all the possible new applications that can be derived by improving the computational efficiency of existing self-supervised learning methods, but their societal impacts will undoubtedly depend on the intended use of the technology.

References

- [1] Sanjeev Arora, Hrishikesh Khandeparkar, Mikhail Khodak, Orestis Plevrakis, and Nikunj Saunshi. A theoretical analysis of contrastive unsupervised representation learning. *arXiv preprint arXiv:1902.09229*, 2019.
- [2] Philip Bachman, R Devon Hjelm, and William Buchwalter. Learning representations by maximizing mutual information across views. In *Advances in Neural Information Processing Systems*, pages 15509–15519, 2019.
- [3] David Berthelot, Nicholas Carlini, Ekin D Cubuk, Alex Kurakin, Kihyuk Sohn, Han Zhang, and Colin Raffel. Remixmatch: Semi-supervised learning with distribution alignment and augmentation anchoring. *arXiv preprint arXiv:1911.09785*, 2019.
- [4] David Berthelot, Nicholas Carlini, Ian Goodfellow, Nicolas Papernot, Avital Oliver, and Colin A Raffel. Mixmatch: A holistic approach to semi-supervised learning. In *Advances in Neural Information Processing Systems*, pages 5050–5060, 2019.
- [5] Mathilde Caron, Piotr Bojanowski, Armand Joulin, and Matthijs Douze. Deep clustering for unsupervised learning of visual features. In *Proceedings of the European Conference on Computer Vision (ECCV)*, pages 132–149, 2018.
- [6] Gal Chechik, Varun Sharma, Uri Shalit, and Samy Bengio. Large scale online learning of image similarity through ranking. *Journal of Machine Learning Research*, 11(Mar):1109–1135, 2010.
- [7] Ting Chen, Simon Kornblith, Mohammad Norouzi, and Geoffrey Hinton. A simple framework for contrastive learning of visual representations. *preprint arXiv:2002.05709*, 2020.
- [8] Sumit Chopra, Raia Hadsell, and Yann LeCun. Learning a similarity metric discriminatively, with application to face verification. In *2005 IEEE Computer Society Conference on Computer Vision and Pattern Recognition (CVPR'05)*, volume 1, pages 539–546. IEEE, 2005.
- [9] Ekin D Cubuk, Barret Zoph, Jonathon Shlens, and Quoc V Le. Randaugment: Practical data augmentation with no separate search. *arXiv preprint arXiv:1909.13719*, 2019.
- [10] Emily Denton, Sam Gross, and Rob Fergus. Semi-supervised learning with context-conditional generative adversarial networks. *arXiv preprint arXiv:1611.06430*, 2016.
- [11] Carl Doersch and Andrew Zisserman. Multi-task self-supervised visual learning. In *Proceedings of the IEEE International Conference on Computer Vision*, pages 2051–2060, 2017.
- [12] Carl Doersch, Abhinav Gupta, and Alexei A Efros. Unsupervised visual representation learning by context prediction. In *Proceedings of the IEEE International Conference on Computer Vision*, pages 1422–1430, 2015.

- [13] Alexey Dosovitskiy, Jost Tobias Springenberg, Martin Riedmiller, and Thomas Brox. Discriminative unsupervised feature learning with convolutional neural networks. In *Advances in neural information processing systems*, pages 766–774, 2014.
- [14] Yueqi Duan, Wenzhao Zheng, Xudong Lin, Jiwen Lu, and Jie Zhou. Deep adversarial metric learning. In *Proceedings of the IEEE Conference on Computer Vision and Pattern Recognition*, pages 2780–2789, 2018.
- [15] Spyros Gidaris, Praveer Singh, and Nikos Komodakis. Unsupervised representation learning by predicting image rotations. *arXiv preprint arXiv:1803.07728*, 2018.
- [16] Jacob Goldberger, Geoffrey E Hinton, Sam T Roweis, and Russ R Salakhutdinov. Neighbourhood components analysis. In *Advances in neural information processing systems*, pages 513–520, 2005.
- [17] Yves Grandvalet and Yoshua Bengio. Entropy regularization. *Semi-supervised learning*, pages 151–168, 2006.
- [18] Michael Gutmann and Aapo Hyvärinen. Noise-contrastive estimation: A new estimation principle for unnormalized statistical models. In *Proceedings of the Thirteenth International Conference on Artificial Intelligence and Statistics*, pages 297–304, 2010.
- [19] Raia Hadsell, Sumit Chopra, and Yann LeCun. Dimensionality reduction by learning an invariant mapping. In *2006 IEEE Computer Society Conference on Computer Vision and Pattern Recognition (CVPR'06)*, volume 2, pages 1735–1742. IEEE, 2006.
- [20] Kaiming He, Haoqi Fan, Yuxin Wu, Saining Xie, and Ross Girshick. Momentum contrast for unsupervised visual representation learning. *arXiv preprint arXiv:1911.05722*, 2019.
- [21] Olivier J Hénaff, Aravind Srinivas, Jeffrey De Fauw, Ali Razavi, Carl Doersch, SM Eslami, and Aaron van den Oord. Data-efficient image recognition with contrastive predictive coding. *arXiv preprint arXiv:1905.09272*, 2019.
- [22] Peter Henderson, Jieru Hu, Joshua Romoff, Emma Brunskill, Dan Jurafsky, and Joelle Pineau. Towards the systematic reporting of the energy and carbon footprints of machine learning. *arXiv preprint arXiv:2002.05651*, 2020.
- [23] Dan Hendrycks, Mantas Mazeika, Saurav Kadavath, and Dawn Song. Using self-supervised learning can improve model robustness and uncertainty. In *Advances in Neural Information Processing Systems*, pages 15637–15648, 2019.
- [24] Elad Hoffer and Nir Ailon. Deep metric learning using triplet network. In *International Workshop on Similarity-Based Pattern Recognition*, pages 84–92. Springer, 2015.
- [25] Prannay Khosla, Piotr Teterwak, Chen Wang, Aaron Sarna, Yonglong Tian, Phillip Isola, Aaron Maschiot, Ce Liu, and Dilip Krishnan. Supervised contrastive learning. *arXiv preprint arXiv:2004.11362*, 2020.
- [26] Alexander Kolesnikov, Xiaohua Zhai, and Lucas Beyer. Revisiting self-supervised visual representation learning. In *Proceedings of the IEEE conference on Computer Vision and Pattern Recognition*, pages 1920–1929, 2019.
- [27] Alex Krizhevsky and Geoffrey Hinton. Learning multiple layers of features from tiny images. *Technical report, University of Toronto*, 2009.
- [28] A. Lacoste, A. Luccioni, Victor Schmidt, and Thomas Dandres. Quantifying the carbon emissions of machine learning. *arXiv preprint arXiv:1910.09700*, 2019.
- [29] Dong-Hyun Lee. Pseudo-label: The simple and efficient semi-supervised learning method for deep neural networks. In *Workshop on challenges in representation learning, ICML*, volume 3, page 2, 2013.
- [30] Junnan Li, Pan Zhou, Caiming Xiong, Richard Socher, and Steven CH Hoi. Prototypical contrastive learning of unsupervised representations. *arXiv preprint arXiv:2005.04966*, 2020.

- [31] Ilya Loshchilov and Frank Hutter. Sgdr: Stochastic gradient descent with warm restarts. *arXiv preprint arXiv:1608.03983*, 2016.
- [32] Geoffrey J McLachlan. *Discriminant analysis and statistical pattern recognition*, volume 544. John Wiley & Sons, 2004.
- [33] Ishan Misra and Laurens van der Maaten. Self-supervised learning of pretext-invariant representations. In *CVPR*, 2020.
- [34] Takeru Miyato, Shin-ichi Maeda, Masanori Koyama, and Shin Ishii. Virtual adversarial training: a regularization method for supervised and semi-supervised learning. *IEEE transactions on pattern analysis and machine intelligence*, 41(8):1979–1993, 2018.
- [35] Mehdi Noroozi and Paolo Favaro. Unsupervised learning of visual representations by solving jigsaw puzzles. In *European Conference on Computer Vision*, pages 69–84. Springer, 2016.
- [36] Aaron van den Oord, Yazhe Li, and Oriol Vinyals. Representation learning with contrastive predictive coding. *arXiv preprint arXiv:1807.03748*, 2018.
- [37] Deepak Pathak, Philipp Krahenbuhl, Jeff Donahue, Trevor Darrell, and Alexei A Efros. Context encoders: Feature learning by inpainting. In *Proceedings of the IEEE conference on computer vision and pattern recognition*, pages 2536–2544, 2016.
- [38] Olga Russakovsky, Jia Deng, Hao Su, Jonathan Krause, Sanjeev Satheesh, Sean Ma, Zhiheng Huang, Andrej Karpathy, Aditya Khosla, Michael Bernstein, Alexander C. Berg, and Li Fei-Fei. Imagenet large scale visual recognition challenge. *International Journal of Computer Vision*, 115(3):211–252, 2015.
- [39] Florian Schroff, Dmitry Kalenichenko, and James Philbin. Facenet: A unified embedding for face recognition and clustering. In *Proceedings of the IEEE conference on computer vision and pattern recognition*, pages 815–823, 2015.
- [40] Abhinav Shrivastava, Abhinav Gupta, and Ross Girshick. Training region-based object detectors with online hard example mining. In *Proceedings of the IEEE conference on computer vision and pattern recognition*, pages 761–769, 2016.
- [41] Jake Snell, Kevin Swersky, and Richard Zemel. Prototypical networks for few-shot learning. In *Advances in neural information processing systems*, pages 4077–4087, 2017.
- [42] Kihyuk Sohn. Improved deep metric learning with multi-class n-pair loss objective. In *Advances in neural information processing systems*, pages 1857–1865, 2016.
- [43] Kihyuk Sohn, David Berthelot, Chun-Liang Li, Zizhao Zhang, Nicholas Carlini, Ekin D Cubuk, Alex Kurakin, Han Zhang, and Colin Raffel. Fixmatch: Simplifying semi-supervised learning with consistency and confidence. *arXiv preprint arXiv:2001.07685*, 2020.
- [44] Ilya Sutskever, James Martens, George Dahl, and Geoffrey Hinton. On the importance of initialization and momentum in deep learning. In *International conference on machine learning*, pages 1139–1147, 2013.
- [45] Yaniv Taigman, Ming Yang, Marc’ Aurelio Ranzato, and Lior Wolf. Deepface: Closing the gap to human-level performance in face verification. In *Proceedings of the IEEE conference on computer vision and pattern recognition*, pages 1701–1708, 2014.
- [46] Yonglong Tian, Dilip Krishnan, and Phillip Isola. Contrastive multiview coding. *arXiv preprint arXiv:1906.05849*, 2019.
- [47] Yonglong Tian, Chen Sun, Ben Poole, Dilip Krishnan, Cordelia Schmid, and Phillip Isola. What makes for good views for contrastive learning. *arXiv preprint arXiv:2005.10243*, 2020.
- [48] Kilian Q Weinberger and Lawrence K Saul. Distance metric learning for large margin nearest neighbor classification. *Journal of Machine Learning Research*, 10(Feb):207–244, 2009.

- [49] Zhirong Wu, Yuanjun Xiong, Stella X Yu, and Dahua Lin. Unsupervised feature learning via non-parametric instance discrimination. In *Proceedings of the IEEE Conference on Computer Vision and Pattern Recognition*, pages 3733–3742, 2018.
- [50] Qizhe Xie, Zihang Dai, Eduard Hovy, Minh-Thang Luong, and Quoc V Le. Unsupervised data augmentation. *arXiv preprint arXiv:1904.12848*, 2019.
- [51] Yang You, Igor Gitman, and Boris Ginsburg. Large batch training of convolutional networks. *arXiv preprint arXiv:1708.03888*, 2017.
- [52] Xiaohua Zhai, Avital Oliver, Alexander Kolesnikov, and Lucas Beyer. S4l: Self-supervised semi-supervised learning. In *Proceedings of the IEEE international conference on computer vision*, pages 1476–1485, 2019.
- [53] Richard Zhang, Phillip Isola, and Alexei A Efros. Colorful image colorization. In *European conference on computer vision*, pages 649–666. Springer, 2016.
- [54] Richard Zhang, Phillip Isola, and Alexei A Efros. Split-brain autoencoders: Unsupervised learning by cross-channel prediction. In *Proceedings of the IEEE Conference on Computer Vision and Pattern Recognition*, pages 1058–1067, 2017.

Recovering Petaflops in Contrastive Semi-Supervised Learning of Visual Representations: Supplementary Material

A Additional details about fine-tuning

We follow the fine-tuning procedure of Chen et al. [7]. Upon completion of pre-training, all methods are fine-tuned on the available labeled data using SGD with Nesterov momentum. We do not employ weight-decay during fine-tuning, and only make use of basic data augmentations (random cropping and random horizontal flipping). The weights of the linear classifier used to fine-tune the encoder network are initialized to zero. On CIFAR10, models are fine-tuned for 90 epochs. All results are reported on the standard CIFAR10 test set. We use a batch-size of 256, along with a momentum value of 0.9 and an initial learning-rate of 0.05 coupled with a cosine-annealing learning-rate schedule. On ImageNet, in the 10% labeled data setting, models are fine-tuned for 30 epochs; in the 1% labeled data setting, models are fine-tuned for 60 epochs. We use a batch-size of 4096, along with a momentum value of 0.9 and an initial learning-rate of 0.8 coupled with a cosine-annealing learning-rate schedule. All results are reported on the standard ImageNet validation set using a single center-crop.

B Limitations

The amount of time that we can leave the SuNCeT loss on without degrading performance is positively correlated with the amount of labeled data. To shed light on this limitation, we conduct experiments on CIFAR10 where we switch-off the SuNCeT loss at a certain epoch, and revert to fully self-supervised

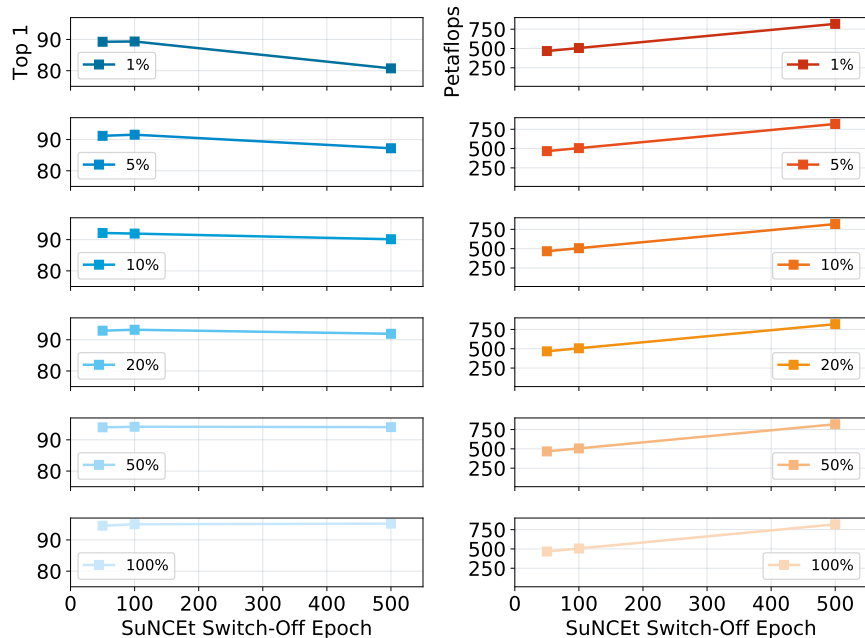


Figure 2: Training a ResNet50 with an adjusted-stem on CIFAR10 given various percentages of labeled data. Left subplots report the final model test-accuracy as a function of the epoch at which the SuNCeT loss is switched off. Right subplots report the amount of petaflops needed to train the corresponding models in the left subplots. The number of epochs that one can utilize the SuNCeT loss for without degrading performance is positively correlated with the amount of available labeled data. To balance improvements in model accuracy with computational costs, it may also be beneficial to switch off the SuNCeT loss early on in training, even if leaving it on does not degrade performance.

learning for the remainder training. All models are trained for a total of 500 epochs; epochs are counted with respect to the number of passes through the unsupervised data loader.

The left subplots in Figure 2 report the final model test-accuracy on CIFAR10 as a function of the switch-off epoch, for various percentages of available labeled data. The right subplots in Figure 2 report the amount of petaflops needed to train the corresponding models in the left subplots.

To study the potential accuracy degradation as a function of the switch-off epoch, we first restrict our focus to the left subplots in Figure 2. When 20% or more of the data is labeled (bottom three subplots), the final model accuracy is relatively invariant to the switch-off epoch (lines are roughly horizontal). However, when less labeled data is available, the final model accuracy can degrade if we leave the SuNCeT loss on for too long (top three subplots). The magnitude of the degradation is positively correlated with the amount of available labeled data (lines become progressively more horizontal from top subplot to bottom subplot).

From a computational perspective, it may also be beneficial to turn off the SuNCeT loss at some point, even if leaving it on does not degrade performance. We hypothesize that once we have squeezed out all the information that we can from the labeled data, it is best to revert all computational resources to optimizing the (more slowly-convergent) self-supervised instance-discrimination task. We see that leaving the SuNCeT loss on for more epochs does not provide any significant improvement in model accuracy (left subplots in Figure 2), but the corresponding computational requirements still increase (right subplots in Figure 2).

In practice we find that switching-off the SuNCeT loss when it has roughly plateaued provides a good strategy for balancing gains in model accuracy with computational costs. We switch off the SuNCeT loss at epoch 100 in all of our CIFAR10 experiments in the main paper (except the experiment with 100% labeled data, where SuNCeT is left on for all 500 epochs of training). Figure 3 depicts the supervised SuNCeT loss during training for various percentages of available labeled data (left subplots), and the self-supervised InfoNCE loss during training for various percentages of available labeled data (right subplots). While the InfoNCE continues decreasing (albeit slowly) for a few

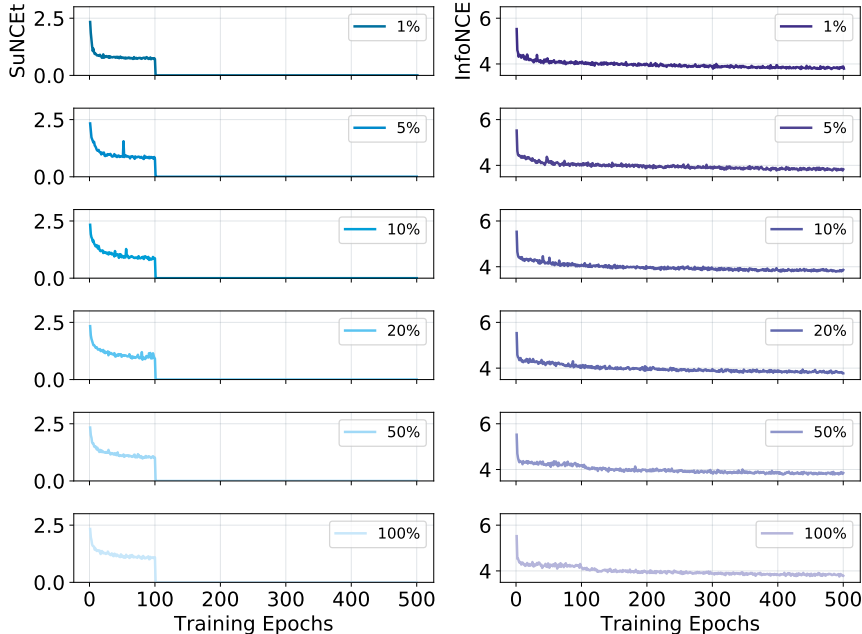


Figure 3: Training a ResNet50 with an adjusted-stem on CIFAR10 given various percentages of labeled data. The SuNCeT loss is only used for the first 100 epochs of training, and then switched off for the remainder of training. Left subplots report the supervised SuNCeT loss during training. Right subplots report the self-supervised InfoNCE loss during training. In practice, we turn off the SuNCeT loss when it has plateaued, and revert to fully self-supervised training thereafter. In these experiments, the SuNCeT loss has roughly plateaued at around 100 epochs of training.

hundred training epochs (right subplots), the SuNCEt loss has roughly plateaued after 100 training epochs (left subplots), and so we switch it off at that point.

Figure 3 also suggests that the rate at which the SuNCEt loss plateaus is negatively correlated with the available amount of labeled data. This observation supports the intuition that one should turn off the SuNCEt loss earlier in training if less labeled data is available (cf. Figure 2).

C Computational accounting

To report the amount of compute used during training we use a pytorch operation-counter tool.³ In particular, we use the tool to compute the number of MACs (multiply-accumulate operations) used to perform a forward pass and evaluate the loss for a given mini-batch. Then we use the formula from <https://www.openai.com/blog/ai-and-compute/> to determine the total number of flops per update

$$\text{flops per update} = (\text{MACs}) * (2 \text{ FLOPs/MAC}) * (3 \text{ for forward and backward pass}).$$

We measure the flops utilized during each update of both pre-training and fine-tuning, and report the aggregate results in petaflops.

D Pseudo-code

Listing 1 provides pseudo-code for integrating the SuNCEt supervised loss with a self-supervised instance discrimination task when a small fraction of labeled data is available during training. The SuNCEt loss is computed on a mini-batch of labeled images and directly added to the instance-discrimination loss.

Listing 1: Pseudo-code for main training script computing InfoNCE+SuNCEt when a small fraction of labeled data is available during training.

```
# -- init image sampler for instance-discrimination
unsupervised_data_loader = ...

# -- init (labeled) image sampler for SuNCEt
supervised_data_loader = ...

for epoch in range(num_epochs):
    for itr, imgs in enumerate(unsupervised_data_loader):
        # -- compute instance-discrimination loss
        z = mlp(encoder(imgs))
        ssl_loss = info_nce(z)

        # -- compute supervised-contrastive loss
        labeled_imgs = next(supervised_data_loader)
        z = mlp(encoder(labeled_imgs))
        supervised_loss = suncet(z)

        # -- compute aggregate loss and update encoder & mlp
        loss = supervised_loss + ssl_loss
        loss.backward()
        optimizer.step()
        lr_scheduler.step()
```

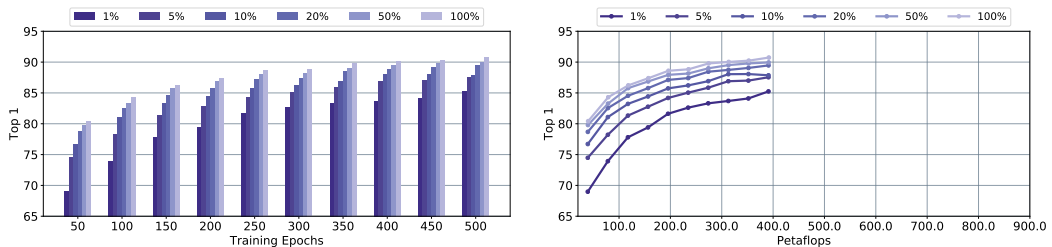
E Linear Evaluation on CIFAR10

For completeness we also evaluate performance when training a linear classifier on top of the *frozen* encoder network using the available labeled data (as opposed to fine-tuning both the encoder network

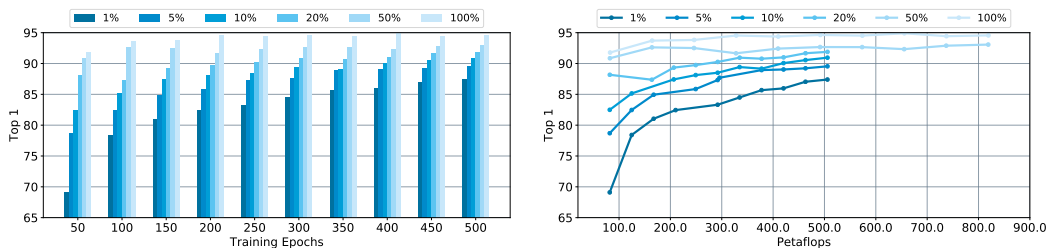
³<https://github.com/Lyken17/pytorch-OpCounter>

and the linear classifier). We switch off the SuNCeT loss after 100 epochs of training in these experiments, except in the cases where either 100% or 50% of the training data is labeled, in which case the loss is left on for the entire 500 epochs of training. We train the linear classifier for 520 epochs using SGD with Nesterov momentum and a batch-size of 256, momentum 0.9, and a step-wise learning rate decay schedule starting at 0.01, and decay to 0.001 and 0.0001 at epochs 480 and 500 respectively. We only make use of basic data augmentations (random cropping and random horizontal flipping) when training the linear classifier.

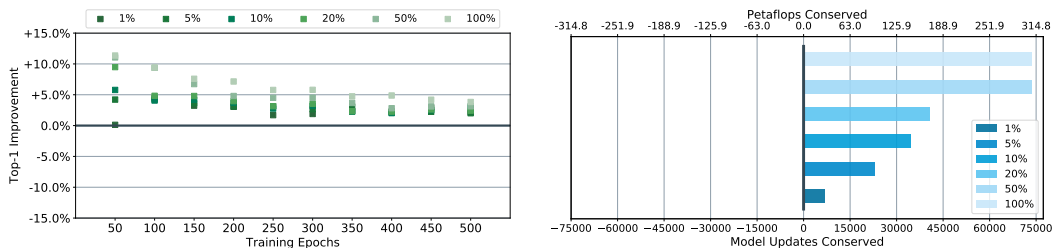
Results. Figure 4a shows the convergence of SimCLR with various amounts of labeled data, both in terms of epochs (left sub-figure) and in terms of computation (right sub-figure). Figure 4b shows the convergence of the SimCLR + SuNCeT combination with various amounts of labeled data, both in terms of epochs (left sub-figure) and in terms of computation (right sub-figure). Figure 4c shows the improvement in Top 1 test accuracy of the linear classifier throughout training (relative to SimCLR) when using SuNCeT. Not only does SuNCeT accelerate training from a sample efficiency point of view (as much as a 10% improvement in test-accuracy within the first 50 epochs, cf. Figure 4c), but it also leads to better models at the end of training. Figure 4d shows the amount of computation saved by the SimCLR + SuNCeT combination in reaching the best SimCLR accuracy. There are two x-axes in this figure. The top shows the petaflops saved and the bottom shows the number of model updates



(a) SimCLR test-set convergence with linear-evaluation on various percentages of labeled data.



(b) SimCLR + SuNCeT test-set convergence with linear-evaluation on various percentages of labeled data.



(c) SuNCeT improvement in test-set convergence with linear-evaluation on various percentages of labeled data. (d) Computation saved by SuNCeT in reaching the best SimCLR test accuracy with linear-evaluation on various percentages of labeled data.

Figure 4: Training a ResNet50 with an adjusted-stem on CIFAR10 given various percentages of labeled data. Evaluations reported at intermediate epochs correspond to checkpoints from the same run, with a 500 epoch learning-rate cosine-decay schedule. SuNCeT epochs are counted with respect to number of passes through the unsupervised data loader.

saved to reach the best SimCLR test accuracy. SuNCEt saves computation for any given amount of supervised samples.